Inorg. Chem. **2007**, *46*, 6864–6870

Synthesis, Structure, and Bonding of $Eu_3Bi(Sn,Bi)_4$. A Rare Inverse-Cr_5B_3-Type Structure with a New Tin/Bismuth Network

Ming-Hui Ge and John D. Corbett*

Ames Laboratory, Department of Energy,[1] and Department of Chemistry, Iowa State University, Ames, Iowa 50011

Received February 12, 2007

The ternary phase $Eu_3Bi(Sn_{1-x}Bi_x)_4$ ($\sim 0 < x < \sim 0.15$) has been synthesized by solid-state methods at high temperature. The crystal structure of the limiting $Eu_3Bi(Sn_{3.39}Bi_{0.61(3)})$ has been determined by single-crystal X-ray analysis to be isopointal with an inverse-Cr_5B_3-type structure [space group *I*4/*mcm*, $Z = 4$, $a = 8.826(1)$ Å, $c = 12.564(3)$ Å, and $V = 978.6(3)$ Å^3]. The structure contains slabs of three-bonded Sn/Bi atoms as puckered eight- and four-membered rings interlinked at all vertices, and these are separated by planar layers of individual Eu and Bi atoms. In the normal (stuffed) Cr_5B_3-type analogue $Eu_5Sn_3H_x$, these two units are replaced by a more highly puckered network of Eu cations around isolated Sn atoms and planar layers of isolated Eu atoms and Sn dimers, respectively. Band structures of limiting models of the phase calculated by TB-LMTO-ASA methods show a metallic character and indicate that the mixed Sn/Bi occupancy in the slabs in this structure for $x > 0$ probably originates with the electronic advantages of the pseudogap that would occur at the electron count of the ideal Zintl phase $Eu_3Bi(Sn_3Bi)$. The stability of a competing phase reduces this limit to $Eu_3Bi(Sn_{3.4}Bi_{0.6})$.

Introduction

Interest in the compounds of main-group elements has been a persistent highlight in solid-state chemistry because of their rich structural varieties and interesting properties. In particular, combinations of main-group p elements with electropositive s-block metals (A = alkali; Ae = alkaline earth) or some rare-earth (R) metals often yield polar compounds (salts) with structures that can be rationalized by Zintl concepts. In these cases, major valence electron transfer from the active metals to p-block elements often generates polyanions that obey octet rules, and the products are usually presumed to be diamagnetic semiconductors.[2] The combination of two p-block elements is an effective way to achieve new anion substructures, such as are found in the large number of more or less classical compounds in the corresponding mixed p-element systems Al−Si, Al−Ge, Sn−Sb, etc.,[3] although in the present group 14/15 system, only the relevant A−Sn−Sb or A−Sn−Bi systems appear to have been studied. Of course, the bonding and properties of Zintl phases may be more complex; some interesting examples turn out to be metallic, and their bonding cannot be explained by simple rules.[4]

Our recent explorations among stannides in the presence of dipositive cations have yielded several novel compounds with unique bonding characteristics, particularly when mixed cations or mixed main-group elements are employed to generate new structure types or to give more electronic flexibility to the polyanions. Cations of different sizes earlier afforded the novel $Ca_{6.2}Mg_{3.8}Sn_7$ with chains of Sn squares,[5] and a more recent example is the electron-rich but pseudo-closed-shell $Ba_2M_2Sn_6$, M = Ca or Yb, with serpentine tin chains that also interact significantly with M.[6] Similarly, a new electronic situation is afforded by mixed main-group elements in the Eu−Sn−Bi system in the present phase $Eu_3Bi(Sn_{1-x}Bi_x)_4$ in which the atom positions are those of an inverse-Cr_5B_3-type structure (space group *I*4/*mcm*). The

* To whom correspondence should be addressed. E-mail: jcorbett@iastate.edu.

(1) This research was supported by the office of the Basic Energy Sciences, Materials Sciences Division, U.S. Department of Energy. The Ames Laboratory is operated for DOE by Iowa State University under Contract DE-AC02-07CH11358.

(2) *Chemistry, Structure and Bonding of Zintl Phases and Ions*; Kauzlarich, S. M., Ed.; VCH Publishers: New York, 1996.

(3) Eisenmann, B.; Cordier, G. In *Chemistry, Structure and Bonding of Zintl Phases and Ions*; Kauzlarich, S. M., Ed.; VCH Publishers: New York, 1996; Chapter 3.

(4) (a) Corbett, J. D. In *Chemistry, Structure and Bonding of Zintl Phases and Ions*; Kauzlarich, S. M., Ed.; VCH Publishers: New York, 1996; Chapter 4. (b) Corbett, J. D. *Angew. Chem., Int. Ed.* **2000**, *39*, 670.

(5) Ganguli, A. K.; Corbett, J. D.; Köckerling, M. *J. Am. Chem. Soc.* **1998**, *120*, 1223.

(6) Ge, M.-H.; Corbett, J. D. *Inorg. Chem.* **2007**, *46*, 4138.

10.1021/ic070281c CCC: $37.00
Published on Web 07/21/2007

only analogous Sn−Bi combinations studied to date appear to be the more classical $K_2[SnBi]$, which contains $(Sn_2Bi_2)^{4-}$ units, and $K_{10}[Sn_2Bi_6]$ with a $Na_{10}Si_2P_6$-type structure in which the anions are $[Sn_2Bi_6]^{10-}$ units built of edge-sharing $SnBi_4$ tetrahedra.[7] The present phase is, to our knowledge, the first Sn−Bi combination in any rare-earth or alkaline-earth metal system.[8]

Cr_5B_3-type structures are exhibited by over 40 binary compositions M_5X_3.[9] The tetragonal structures (*I*4/*mcm*) contain equal portions of isolated and dimerized anions (dumbbells) in the relevant family of alkaline-earth (Ae) and divalent rare-earth (R) metal tetrelides A_3Tt_5 (Tt = Si−Pb). These were first assessed as Zintl phases $[(Ae^{2+})_5Tt_2^{6-}Tt^{4-}]$, but many were later found to be metallic and without such electronically simple dianions, and some were actually ternary hydrides.[10,11] In addition, In_5Bi_3,[12] Tl_5Te_3, and Tl_5Se_3,[13] which are isopointal with Cr_5B_3 (*I*4/*mcm*), exhibit very different cell proportions from other examples, and they also lack dimers. These effects have led to a division of the so-called Cr_5B_3-type family into two subfamilies according to their *c*/*a* ratios.[13] The major Cr_5B_3-type subgroup is characterized by *c*/*a* ratios of ∼1.76−1.96, and the minor In_5Bi_3 subfamily, by smaller values of around 1.45. Some ternary derivatives are also known in the In_5Bi_3 branch, mostly for Tl_5Te_3, e.g., $PbTl_4Te_3$, $BiTl_9Te_6$, $SbTl_9Te_6$, some of which crystallize in other space groups *I*4/*m*, *P*4/*ncc*, or *Ibam*.[13] Presumably, the In_5Bi_3 subgroup members are notably less polar in their bonding than the majority.

In contrast to the large number of compounds with Cr_5B_3-type structures, inverse-Cr_5B_3 types are very rare. To date, only La_3GeIn_4[14] and $R_3(Ga_{\sim 2}Ge_{\sim 3})$ (R = Tm, Lu)[15] have been reported with this structure. Both have *c*/*a* values comparable to those of the In_5Bi_3 subfamily, but this result appears to be unrelated. We here report the synthesis of a third inverse example, $Eu_3Bi(Sn_{1-x}Bi_x)_4$ over a composition range, and the single-crystal refinement of $Eu_3Bi(Sn_{3.4}Bi_{0.6})$. The electronic bonding requirements of the phase are also analyzed by means of ab initio TB-LMTO-ASA calculations.

Experimental Section

Syntheses. $Eu_3Bi(Sn_{1-x}Bi_x)_4$ samples were prepared by solid-state reactions of the elements Eu (99.9%, Ames Laboratory), Bi (99.999%, Alfa-Aesar), and Sn (99.9%, Alfa-Aesar). All manipulations were performed in nitrogen-filled gloveboxes with moisture levels below 0.1 ppm. Each sample was loaded into a tantalum container that was subsequently arc-welded shut under an argon atmosphere and then sealed in an evacuated silica tube. Samples were first heated to 940 °C, held for 12 h, then cooled to 800 °C at 10 °C/h and held there for 168 h, and finally slowly cooled to room temperature. Reactions were also run under a dynamic vacuum condition to exclude any possible hydride problems, and the same products were obtained.

Table 1. Inverse-Cr_5B_3-Type Phases Studied

loaded composition	refined composition	lattice dimens		
		a, Å	*c*, Å	*V*, Å^3
$Eu_2SrSn_3Bi_2$[a]	$Eu_{2.5}Sr_{0.5}Bi(Sn_{3.4}Bi_{0.6})$	8.855(1)	12.638(3)	990.9(3)
$Eu_3Sn_{4.5}Bi_{0.5}$[b]	none	8.781(1)	12.438(3)	959.1(3)
Eu_3Sn_4Bi[a]	$Eu_3Bi(Sn_{3.99}Bi_{0.01})$	8.803(1)	12.455(3)	965.1(3)
$Eu_3Sn_3Bi_2$[a]	$Eu_3Bi(Sn_{3.39}Bi_{0.61})$	8.826(1)	12.564(3)	978.6(3)
$Eu_3Sn_2Bi_3$	other phases			
Eu_3SnBi_4	other phases			

[a] Lattice dimensions from single-crystal data. [b] Lattice dimensions from the selected powder diffraction peaks.

Preliminary investigations of possibly related compounds in the Sr−Sn−Bi, Yb−Sn−Bi, and Ba−Sn−Bi systems revealed only other types of products. A Sr_3Sn_4Bi composition yielded a novel compound $Sr_{11}Sn_{12}Bi_4$.[16] Yb_3Sn_4Bi and Ba_3Sn_4Bi compositions produced $(Yb,Ba)_{11}Sn_2Bi_8$ phases with $Ho_{11}Ge_{10}$-type structures as well as Ba_3Sn_5[17] with a Pu_3Pd_5-type structure in the latter system and other unknown phases. The title phase did not form with Pb or with Sb. Experiments in the Sr−Eu−Sn−Bi system showed that the cations could be mixed but only for a relatively small amount of Sr, ∼25% according to a single-crystal refinement.

Powder X-ray Diffraction and Phase Analyses. Powder X-ray diffraction patterns were obtained from samples mounted in the glovebox between pieces of Mylar so as to protect them from the atmosphere. A Huber 670 Guinier Powder camera equipped with an area detector and Cu Kα radiation (λ = 1.540 598 Å) was employed to obtain quality data. (Lattice constants generally agreed with those from the Bruker diffractometer within a few σ for the separate values.) The reported phase was first detected in the products of an exploratory synthesis with the composition $Eu_2SrSn_3Bi_2$. Several single crystals were obtained from this, all of which crystallized with an inverse-Cr_5B_3-type structure. After the structural analysis was completed, a series of reactions with only Eu as the cation were conducted to obtain useful crystals and some idea of any phase width.

The selection of data given in Table 1 suggests some composition variability. First, powder X-ray analyses of the products showed that a $Eu_3Bi(Sn_{1-x}Bi_x)_4$ phase formed for the loaded compositions $Eu_3Sn_{4.5}Bi_{0.5}$, Eu_3Sn_4Bi, and $Eu_3Sn_3Bi_2$. However, no such pattern was found with $Eu_3Sn_2Bi_3$ and Eu_3SnBi_4 compositions, rather a $Ho_{11}Ge_{10}$-type phase. The target phase constituted up to 80% for the loaded composition $Eu_3Bi(Sn_4Bi_0)$ in terms of the relative X-ray scattering powers but only about 20% for $Eu_3Sn_{4.5}Bi_{0.5}$. Therefore, the composition within the $Eu_3Bi(Sn_{1-x}Bi_x)_4$ phase is probably in the range of $0 < x < 1$ or perhaps somewhat into a negative *x* range. (Linear extrapolation of the cell volumes suggests on the order of 25% substitution of Sn into the 4*c* Bi position in the second Bi-poor sample listed, but no single crystals were located.) Several single crystals were obtained from the Eu_3Sn_4Bi and $Eu_3Sn_3Bi_2$ reactions. Although the exact solid solution range has not been determined, refinements of data from these two showed that mixed Sn/Bi occupancies occur only on the 16*l* positions and no other.

(7) (a) Asbrand, M.; Eisenmann, B. *Z. Naturforsch.* **1996**, *51b*, 1301. (b) Asbrand, M.; Eisenmann, B. *Z. Kristallogr.* **1993**, *205*, 323.
(8) ICSD: Fachinformationszentrum, Karlsruhe, Germany, and the National Institute of Standards and Technology, Washington, DC, 2006.
(9) Villars, P.; Calvert, L. D. *Pearson's Handbook of Crystallographic Data for Intermetallic Phases*, 2nd ed.; American Society for Metals International: Metals Park, OH, 1991.
(10) Leon-Escamilla, E. A.; Corbett, J. D. *Inorg. Chem.* **2001**, *40*, 1226.
(11) Mudring, A.-V.; Corbett, J. D. *J. Am. Chem. Soc.* **2004**, *126*, 5277.
(12) Kubiak, R. *Z. Anorg. Allg. Chem.* **1977**, *431*, 261.
(13) Böttcher, P.; Doert, Th.; Druska, Ch.; Bradtmöller, S. *J. Alloys Compd.* **1997**, *246*, 209.
(14) Guloy, A. M.; Corbett, J. D. *Inorg. Chem.* **1996**, *35*, 2616.
(15) Venturini, G.; Welter, R. *J. Alloys Compd.* **2000**, *299*, L9.
(16) Ge, M.-H.; Corbett, J. D., unpublished research.
(17) Klem, M. T.; Vaughey, J. T.; Harp, J. G.; Corbett, J. D. *Inorg. Chem.* **2001**, *40*, 7020.

Table 2. Summary of Some Data Collection and Structure Refinement Parameters for $Eu_3Bi(Sn_{3.39}Bi_{0.61(3)})$

empirical formula	$Eu_3Sn_{3.39}Bi_{1.61}$
fw	1193
space group, Z	I4/mcm (No. 140), 4
unit cell parameters (Å)	
a	8.826(1)
c	12.564(3)
c/a	1.424
volume (Å^3)	978.6(3)
density (Mg/m^3)	8.098
μ(Mo Kα) (mm^{-1})	55.905
measured/ indep. obs. refl.	1990/202
R1, wR2 (all data)	0.0178, 0.0377

For the former Sn-richer sample, two refinements of single-crystal data from the $Eu_3Bi(Sn_4Bi_0)$ product revealed a composition Eu_3BiSn_4 (details in Table 1 and the Supporting Information) with substantially pure Sn on site 16*l*. In detail, the mixed Sn2/Bi2 occupancy at 16*l* was 0.99/0.01(1), and for the Bi1/Sn1 4*c* site, 0.97/0.03(2). Both sites are therefore single element statistically. For loaded $x = 0.25$, $Eu_3Bi(Sn_3Bi)$, several single-crystal data sets yielded compositions of around $Eu_3Bi(Sn_{3.4}Bi_{0.6})$ [$=Eu_3Bi(Sn_{0.85}Bi_{0.15})_4$], and the other major product was a $Ho_{11}Ge_{10}$-type phase. The former should represent the Bi-rich limit, making $0 < x < 0.15$. (More details appear in the crystallography section below.)

Energy-Dispersive X-ray (EDX) Spectroscopy. EDX analyses of six single crystals picked from products of loaded reactions $Eu_3Sn_3Bi_2$ and Eu_3Sn_4Bi all confirmed the presence of Eu, Sn, and Bi, $\sim Eu_3Sn_{3.6}Bi_{1.2}$ in the former. Sr was also present in single crystals from the $(Eu,Sr)_3(Sn,Bi)_5$ reaction.

Single-Crystal Structural Studies. A silver-gray crystal (0.09 × 0.15 × 0.20 mm^3) was selected from the products of a loaded composition $Eu_3Sn_3Bi_2$ and was sealed into a thin-walled glass capillary under nitrogen. Data collection was performed on a SMART APEX CCD diffractometer (Mo Kα radiation, graphite monochromator) at 293 K. Initial cell constants and an orientation matrix for data collection were determined from the least-squares refinement of the setting angles of 25 centered reflections. (Final lattice constants were generally within 0.01 Å of the Huber result for 10−15 Å axial lengths.) The diffraction data were corrected for Lorentz and polarization effects and for absorption with *SADABS*.[18] The space group was determined to be *I*4/*mcm* on the basis of systematic absences, *E*-value statistics, and the satisfactory refinement of the structure. The structure was solved by direct methods (*SHELXS*), which revealed all Eu, Sn, and Bi atoms. The structure was refined by least-squares methods on F^2, ultimately with anisotropic displacement parameters, with the aid of the *SHELXTL* package.[19] Further refinements suggested that three sites were fully occupied by single atom types, whereas the 16*l* site (Sn/Bi2) had a mixed occupancy. Final difference Fourier maps showed featureless residual peaks of +1.532 and −1.069 e/Å^3. The parameters for data collection and refinement are summarized in Table 2, the atomic coordinates and isotropic displacement parameters are listed in Table 3, and the main interatomic distances are given in Table 4. More details regarding the crystallographic studies and anisotropic displacement parameters appear in the Supporting Information (CIF).

Theoretical Calculations. The band structures for the compositions $Eu_3Bi(Sn_{1-x}Bi_x)_4$, $x = 0$ and 0.25, were calculated according to TB-LMTO-ASA methods with the aid of the Stuttgart LMTO 47 program.[20] No interstitial spheres were necessary within the 18% overlap default. The Eu 4f orbitals were treated as core levels. An ordered distribution of Sn and Bi in $P\bar{1}$ symmetry was utilized for the latter calculation.

Table 3. Atomic Coordinates (× 10^4) and Isotropic Equivalent Displacement Parameters (Å^2 × 10^3) for $Eu_3Sn_{3.39}Bi_{1.61(3)}$

	Wyckoff	x	y	z	U(eq)	sof
Eu1	4*a*	0	0	2500	10(1)	1.00
Bi1	4*c*	0	0	0	12(1)	1.00
Eu2	8*h*	3399(1)	8399(1)	0	12(1)	1.00
Sn/Bi(2)	16*l*	1437(1)	6437(1)	1861(1)	12(1)	0.848/0.152(8)

Table 4. Selected Interatomic Distances for $Eu_3Bi(Sn_{3.39}Bi_{0.61(3)})$

atom 1	atom 2	d (Å)	atom 1	atom 2	d (Å)
Eu1	2 Bi1	3.1410(6)	Bi1	2 Eu1	3.1410(6)
	8 Sn/Bi	3.4844(7)		4 Eu2	3.3159(6)
Eu2	2 Bi1	3.3159(6)	Sn/Bi	4 Sn/Bi	3.002(2)
	2 Sn/Bi	3.386(2)		2 Sn/Bi	3.102(2)
	4 Sn/Bi	3.560 (1)		Eu2	3.386(2)
	Eu2	3.996 (1)		2 Eu1	3.4844(7)
				2 Eu2	3.560(1)

Results and Discussion

Structure Description. Tetragonal $Eu_3Bi(Sn_{1-x}Bi_x)_4$, $\sim 0 \leq x \leq \sim 0.15$, represents the third example of an inverse-Cr_5B_3-type structure. In this instance, we can make a useful and direct comparison with the structure that has been refined for Eu_5Sn_3H, a normal Cr_5B_3-type that is stable for these two metals only as the stuffed hydride.[10] The basics of the two structures are illustrated in Figure 1 in views along ~-[100] and in Figure 2 in projections roughly along [001]. The contrasts are emphasized by heavier red lines that mark bonds (closer interactions) in each, together with thin black lines that mark former interatomic bonds in the other type. The numbers (in angstroms) relate distances that change markedly during this interconversion.

The structure of $Eu_3Bi(Sn_{3.4}Bi_{0.6})$ (Figure 1a) can be described in terms of puckered $Eu(Sn_{3.4}Bi_{0.6})$ slabs centered around $z = (1/4, 3/4)$ that alternate along the c direction (vertical) with Eu_2Bi layers of separate Eu2 and Bi1 atoms at $z = (0, 1/2)$. The $Eu(Sn/Bi)_4$ slab is defined by Sn/Bi atoms in a single 16*l* site that generate a puckered $^{85}/_{15}$ Sn/Bi network made up of eight-membered rings centered by Eu1 and interconnected via four-membered rings (flattened tetrahedra) at all vertices (compare Figure 2a). All of the Sn/Bi atoms are three-bonded, and the overall array can be described as antisymmetric pairs of 3^2434 nets separated by intervening mirror planes, $(x, y, 1/2)$, for instance. The distances within the four-membered rings are 3.003(2) Å, and in the eight-membered rings, alternating values of 3.102-(2) Å and the common 3.003 Å. The internal angles in the four- and eight-membered rings are 73.37(3)° and 103.55-(2)°, respectively. These Sn−Sn distances are consistent with other three-bonded examples, for instance, 3.044 Å in $SrSn_4$[21] and 3.00 Å in the base of the approximately square-pyramidal anion in (metallic) Ae_3Sn_5 (Ae = Sr, Ba).[17,22] Single bond Bi−Bi distances would be longer, such as the 3.22, 3.27,

(18) Blessing, R. H. *Acta. Crystallogr.* **1995**, *A51*, 33.
(19) *SHELXTL*; Bruker AXS, Inc.; Madison, WI, 2000.
(20) Tank, R.; Jepsen, O.; Burckhardt, H.; Andersen, O. K. *Program TB-LMTO* 47; Max-Plank-Institut für Festkörperforschung; Stuttgart, Germany, 1994.
(21) Hoffmann, S.; Fässler, T. F. *Inorg. Chem.* **2003**, *42*, 8748.

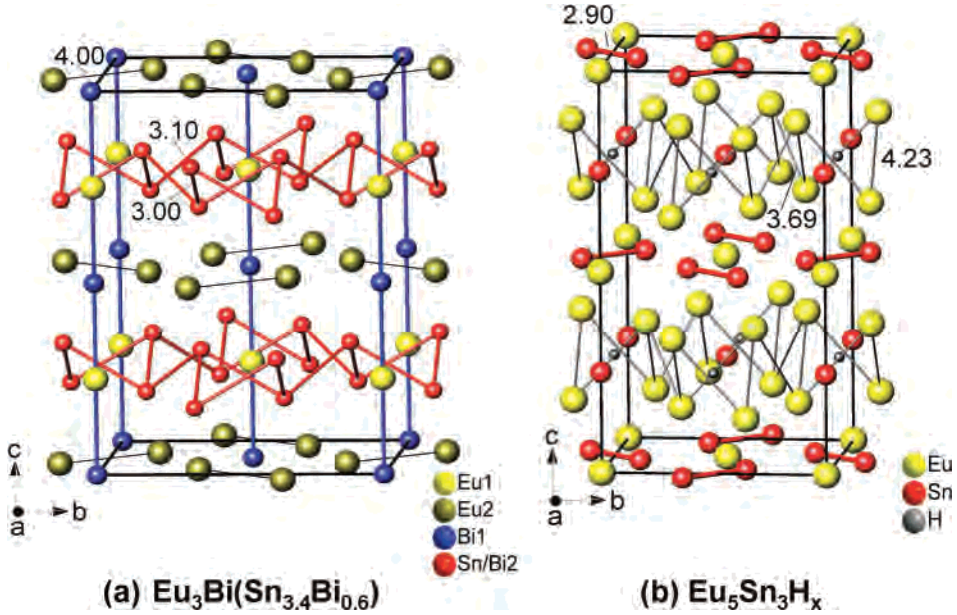

Figure 1. Crystal structure of (a) $Eu_3Bi(Sn_{3.4}Bi_{0.6})$ (inverse-Cr_5B_3-type) and (b) $Eu_5Sn_3H_x$ (Cr_5B_3-type) viewed along ~[100]. Distances (Å) mark what are important bonds (red) in one structure and the corresponding large interatomic separations (light lines) in the other.

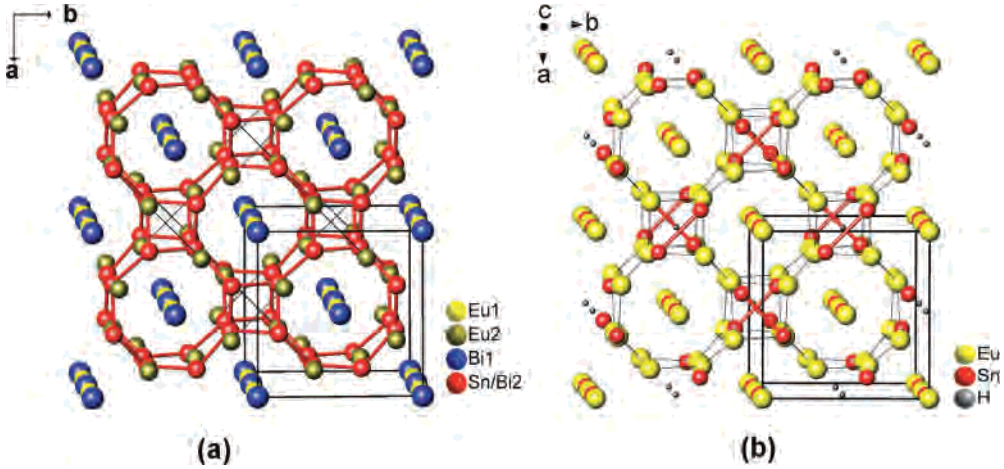

Figure 2. Sn/Bi network in a ~[001] view in tetragonal (a) $Eu_3Bi(Sn_{3.4}Bi_{0.6})$, and (b) $Eu_5Sn_3H_2$. The Eu2 (olive) atoms alternate with Sn/Bi2 (red) in the slabs along *c* in the former and, likewise, Sn (red) alternates with Eu (yellow) in the "slabs" along *c* in the latter.

and 3.29 Å distances in the formal Bi^- chain in $EuBi_2$[23] and in the Bi_4^{4-} squares and Bi_2^{4-} dumbbells in $Sr_{11}Bi_{10}$,[24] respectively. Clearly, Sn/Bi−Sn/Bi distances of 3.00 and 3.10 Å in the title compound are reasonable for an 85% Sn occupancy.

Important bonding relationships also exist between the Eu2−Bi1 layer and the Sn/Bi2−Eu2 slabs, as would be expected. Eu1 and Bi1 alternate along (0, 0, *z*) with a separation of 3.141 Å (*c*/4), whereas (as noted before[14]) the Eu2 atoms in the planar layer lie nearly directly below and above Sn/Bi2 atoms on the far sides of the adjoining puckered layers, as can be perceived in Figure 2a and in part of the Eu2 local environment illustrated in Figure 3. This gives Eu2 three closer Sn/Bi neighbors in each of the two adjoining slabs at 3.386(2) and 3.560(1) (×2) Å. The Eu alignment is close to ideal, with the angle Sn/Bi−Eu−Sn/Bi being 174°, but the $[Sn(Bi)]_3$ triangles are appreciably

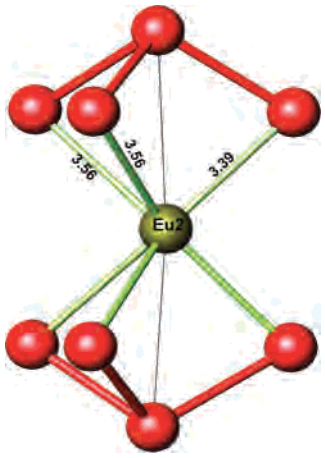

Figure 3. Interslab orientation and distances between Eu2 and the adjoining Sn/Bi puckered layers. The extreme angle is ~174°.

(22) Zürcher, F.; Nesper, R.; Hoffmann, S.; Fässler, T. F. *Z. Anorg. Allg. Chem.* **2001**, *627*, 2211.
(23) Sun, Z.-M.; Mao, J.-G. *J. Solid State Chem.* **2004**, *177*, 3752.
(24) Derrien, G.; Tillard-Charbonnel, M.; Manteghetti, A.; Monconduit, L.; Belin, C. *J. Solid State Chem.* **2002**, *164*, 169.

distorted, with internal angles that differ by 24°. The above Eu−Sn/Bi distances are comparable to those in the slabs, 3.484(1) Å.

Mixed-atom occupancies of the 16*l* site in the title compound range between 15% Bi (85% Sn) and essentially zero Bi. In the earlier inverse example, La_3GeIn_4,[14] substitution of up to 75% of the neighboring Sn for In in the same 16*l* site still provided high yields of the same structure and with no involvement at the 4*c* Ge site. The final product was still Pauli-like in its magnetic susceptibility and hence evidently metallic but much less so than with one less Sn. (It should be remembered that such compositional variations, or the lack of the same, may be critically dependent on the stabilities of alternate phases as well.)

Comparable variations in compositions for the isotypic $Tm_3Ge(Ge_{\sim 2}Ga_{\sim 2})$ are probably also possible. However, the latter mixed Ga/Ge distributions were naturally not quantified in the single-crystal X-ray study; rather 100% Ge in the 4*c* site and a 50/50 Ga/Ge proportion in the 16*l* position were assumed.[15] That composition fell within the range of EDX analyses obtained for this phase in (nonequilibrium) samples in which it was admixed with four other phases, but the existence of a composition range was not considered.

Structure Comparisons. The similarities of and distinctions between the antitypes $Eu_3Bi(Sn_{3.4}Bi_{0.6})$ versus $Eu_5Sn_3H_x$ are readily judged from the comparisons in Figures 1 and 2. Both crystallize in the same body-centered tetragonal system (*I*4/*mcm*) and with the same four independent crystallographic sites occupied, but the antitype relationship means that the stoichiometric proportions (3:5 vs 5:3), the roles of the so-called cations and anions, and important covalent bonding relationships are all reversed. Thus, position types and numbers for Eu here take on former isolated and dimeric Sn functions, whereas the present Sn/Bi (16*l*) and Bi (4*c*) positions relate to earlier Eu-only functions (or of M^{2+} in other isotypes). Perhaps the most prominent feature of this particular A_5Tt_3 family is the presence of dimers of the tetrel element, $(Sn2)_2$ in this case (d = 2.88 Å), whereas each of the equivalent Eu2 atoms here has undergone a displacement of over 0.5 Å in the $x-y$ plane to eliminate the dimer feature. This not only reduces what would otherwise be a strong intercation repulsion but also allows more favorable alignment of Eu2 with Sn/Bi atoms in the adjacent puckered anionic slabs (Figure 3). Likewise, clear repulsions between Eu cations in the puckered slabs of 16*l* Eu in the 5:3 phase (which are held together by isolated Sn1 anions) are replaced by a *bonded* Sn/Bi polyanionic layer now centered by Eu1. This alteration clearly decreases the thickness of each puckered layer by 1.42 Å, from 3.024 Å in $Eu_5Sn_3H_x$[10] to 1.606 Å in $Eu_3Bi(Sn_{3.4}Bi_{0.6})$. The compactness between the slabs also increases, as can be judged from the decreased distances between the atoms that alternate along (0, 0, z), 3.77 Å for Eu1−Sn1 in $Eu_5Sn_3H_x$ versus 3.141 Å for Bi1−Eu1 in the antitype, even though the intrinsic anionic radii of the p elements presumably increase from Sn to Bi. These collective effects are clearly responsible for the correspondingly smaller values for c/a in these three inverse-Cr_5B_3-type phases, 1.424 here, 1.445 in La_3GeIn_4, and 1.398 in $Tm_3Ge(Ge_{\sim 2}Ga_{\sim 2})$ versus a fairly normal c/a = 1.84 for $Eu_5Sn_3H_x$. This characteristic of inverse-Cr_5B_3-type structures has nothing to do with the presence of similarly low c/a values for what has been labeled the In_5Bi_3 subgroup among standard Cr_5B_3-type examples.[13]

Bonding. Bonding in this small group of inverse-Cr_5B_3-type compounds is additionally interesting because the three have similar electron counts, and two are known to be stable into electron-poorer regions insofar as Zintl formulations and simple octet criteria are concerned. Furthermore, the present Bi-richer result has a Fermi energy close to a consistent pseudogap in the densities-of-states (DOS), one that, in fact, corresponds to the electron count of the ideal Zintl phase (below). Thus, these pseudogaps represent more reality in those situations in which a Zintl phase composition pertains, but the phase still has a nonzero DOS at E_F and a metallic conduction. The title phase has 27.4 valence (p) electrons at the Bi-rich limit (e/a = 3.42), ∼0.6 electrons short [3(2)−3−3.6(1)] for an ideal Zintl phase (28e). (Eu^{II} is assumed; the oxidizing Eu^{III} would be very unlikely in the presence of anionic Sn and Bi states.) The similar La_3GeIn_4 (25e) is three electrons short, but further investigations at the same time showed that Sn could be substituted for 16*l* In with high yields up through $La_3GeInSn_3$, at which point the composition is ideal and precise.[14] In fact, this limiting sample is evidently a poor metal, fairly typical for nominal Zintl phases of these and earlier elements.[4] (Only 2D EHTB calculations were made on the isolated In_4^{5-} layer in La_3GeIn_4, and these indicated a notable gap at 28e, a common overestimate with this method and model. The assigned composition $Tm_3Ge(Ge_{\sim 2}Ga_{\sim 2})$ is only 0.7e deficient, but this is presumably a coincidence.)

To better understand the chemical bonding in $Eu_3Bi(Sn_{1-x}Bi_x)_4$, several calculations were performed according to TB-LMTO-ASA methods.[20] Electronic band structures were calculated for three compositions to clarify the above problems: first, for "$Eu_3Bi(Sn_4Bi_0)$" containing only Sn on site 16*l* and, second, on the hypothetical limit "$Eu_3Bi(Sn_3Bi)$" (in reduced $P\bar{1}$ symmetry) with (ordered) 3:1 Sn/Bi on what were formerly 16*l* sites. These two examples straddle the experimental upper (electron-richer) Sn/Bi limit in 16*l*, 85:15. Finally, the composition $Eu_3Bi(Sn_{3.5}Bi_{0.5})$ with a 7:1 ordered mixture gave a close approximation to the experimental value of 3.6:0.4 and a close match of the gap and E_F (not shown).

The first two band structure calculations exhibited the characteristics of a metallic phase, consistent with the simple electron counting. For Eu_3BiSn_4, Figure 4a, E_F cuts the shoulder of the valence band at 108e, below the DOS minimum of ∼112e (Z = 4), whereas the results for the $Eu_3Bi(Sn_3Bi)$ equivalent put the Fermi level very slightly above the calculated DOS minimum and at the ideal 112e (Figure 4b). These results clearly show the advantages of a rational Sn/Bi mixing that takes the system closer to the pseudogap. That the ideal composition slightly exceeds the experimental limiting composition probably occurs because the actual limit is determined by the relative thermodynamic stabilities of competing phase(s) in equilibrium at that point, the observed

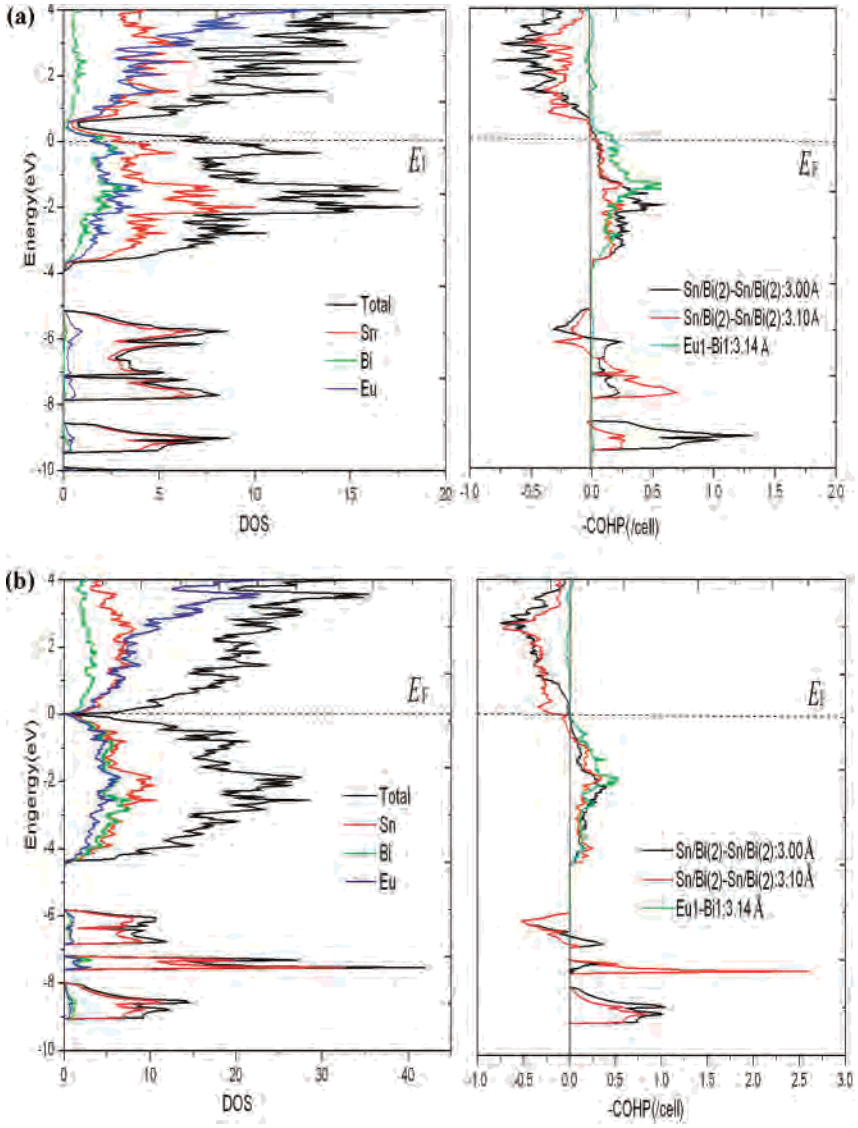

Figure 4. Graphical representation of the results of TB-LMTO-ASA for (a) $Eu_3Bi(Sn_4)$ and (b) $Eu_3Bi(Sn_3Bi)$. The projected DOS (PDOS) are Sn (red), Bi (green), and Eu (blue) (left). The crystal orbital Hamiltonian population (−COHP) plots (right) pertain to the two independent bond distances between Sn/Bi(2) atoms in the layers (black, red) and to Eu1−Bi1 bonds along *c* (green). The Fermi levels are at 108 and 112 e/cell, respectively.

$Eu_{11}(Sn,Bi)_{10}$ ($Ho_{11}Ge_{10}$ type[25]) in particular, not by the electronic structure alone. In both models, Sn, Bi, and Eu show appreciable contributions to the DOS near the Fermi level (Figure 4a). This is in agreement with the presence of clear Sn/Bi−Sn/Bi bonding in the layers and considerable Eu−Bi interaction along the *c* axis, especially near E_F, as follows.

To better quantify the interactions between atoms, crystal orbital Hamilton population (−COHP) data were also evaluated (Figure 4, right). At the Fermi level, Sn/Bi(2)−Sn/Bi(2) bonding (3.00 and 3.10 Å) are both optimized in model a, whereas the Eu1−Bi1 data show that some bonding character still remains. The Eu 5d and Sn 5p orbitals make the principal contributions there, in parallel with recent results for $EuGe_2$[26] as well as for d orbital participation from alkaline-earth metals in some Ae_5Tt_3 examples,[11] Ba(Mg,-In)$_8$,[27] and so forth. To quantify the interactions between atoms, integrated populations (−ICOHP) were also determined. (−ICOHPs obtained from the first-principle LMTO methods are better measures of relative bond strengths than Mulliken overlap populations from extended Hückel methods.) Those for Sn/Bi−Sn/Bi (3.00 Å), Sn/Bi−Sn/Bi (3.10 Å), and Eu1−Bi1 (3.14 Å) (Figure 4b) are about 1.32, 0.70, and 0.86 eV/bond·mol, respectively, indicating very substantial total Eu−Bi bonding along *c* as well as Sn−Sn bonding in the networks. Thus, it is important that the relatively short Eu−Bi interlayer bonds not be ignored. In addition, Eu1,2−Sn/Bi interactions also remain bonding well above E_F (figures in the Supporting Information).

Such analyses are also useful in providing more insights into how and why nominal Zintl phases may coincidentally also remain metallic and how they may be tuned.

(25) Smith, G. S.; Johnson, Q.; Tharp, A. G. *Acta. Crystallogr.* **1967**, *23*, 640.

(26) Bobev, S.; Bauer, E. D.; Thompson, J. D.; Sarrao, J. L.; Miller, G. J.; Eck, B.; Dronskowski, R. *J. Solid State Chem.* **2004**, *177*, 3545.

(27) Bin, L.; Corbett, J. D. *Inorg. Chem.* **2007**, *46*, 2237.

Conclusions

The tetragonal phase $Eu_3Bi(Sn_{1-x}Bi_x)_4$, only the third example of a rare inverse-Cr_5B_3-type structure, exhibits new layered substructures, three-bonded Sn/Bi slabs of puckered eight- and four-membered rings interlinked at all vertices that are separated by planar layers of individual Eu and Bi atoms. The upper x limit, 0.15, lies close to the ideal Zintl phase composition ($x = 0.25$) electronically, but the phase remains a poor metal. Notably more bonding interactions appear to be present in this phase versus the normal antitypic $Eu_5Sn_3(H_x)$. The nonstoichiometric variations observed in the puckered layers in both the title phase and the published isotypic La_3GeIn_4[14] allow closer approaches to the ideal Zintl compositions, but the title phase exhibits only a sizable pseudogap at that point and retains metallic characteristics. Cation d orbital contributions appear important in the states present at the ideal gap.

Acknowledgment. The authors thank Gordon J. Miller and Bin Li for advice on the calculations.

Supporting Information Available: Refinement parameters for $Eu_3Bi(Sn_{3.6}Bi_{0.4})$ in CIF format; tables of additional crystallographic and refinement parameters for $Eu_3Bi(Sn_4Bi_0)$; three figures of −COHP data for separate Eu−Sn/Bi contacts, an amplified DOS plot around E_F, and a projection of Eu d orbitals in the DOS, all for the model $Eu_3Bi(Sn_4Bi_0)$. This material is available free of charge via the Internet at http://pubs.acs.org.

IC070281C